

Surprisingly great difference in reactivity depending upon the ring size: solvolysis and molecular structure study of some *N*-trimethylsilylated cyclic ureas

Roland Szalay^{a,*}, Gábor Pongor^b, Veronika Harmat^c, Zsolt Böcskei^b, Dezső Knausz^a

^a Department of General and Inorganic Chemistry, Eötvös Loránd University, 112 P.O. Box 32, H-1518 Budapest, Hungary

^b Department of Theoretical Chemistry, Eötvös Loránd University, 112 P.O. Box 32, H-1518 Budapest, Hungary

^c Protein Modeling Research Group, Hungarian Academy of Sciences, Eötvös Loránd University, 112 P.O. Box 32, H-1518 Budapest, Hungary

Received 30 September 2004; accepted 15 December 2004

Available online 22 January 2005

Abstract

The molecular structure of *N*-trimethylsilylated five- (**1a–c**), six- (**2a,b**) and seven-membered (**3**) cyclic ureas was studied by single crystal X-ray diffraction method and quantum chemical calculations. Solvolysis rate constants of compounds in *n*-octanol/tetrahydrofuran mixtures were determined by gas chromatography. An alternative sampling method eliminating the effect of the hot injector was also developed in the rate measurement of **2a**. The half-lives of the five-membered rings (**1a,b**) were found to be at least three orders of magnitude higher than those of the six- (**2a,b**) and seven- (**3**) membered ones. Relationship between the reactivity and the extent of the pseudo-pentacoordination around the silicon centre in reactants was found. The results are in correlation to our simple static (structure-based) predictive model established previously.

© 2005 Elsevier B.V. All rights reserved.

Keywords: Silyl; Urea; Pseudo-pentacoordination; Solvolysis; Reactivity

1. Introduction

Silylated carboxamide derivatives, e.g. *N,O*-bis(trimethylsilyl)acetamide (BSA), *N,N'*-bis(trimethylsilyl)urea (BSU), *O*-trimethylsilyl *N,N*-dimethylcarbamate (DMCTMS), are extensively employed as silylating reagents both in organic syntheses and in analytical applications (gas chromatography, mass spectrometry) [1]. In order to carry out the silylation reaction in a chemo-, regio- or stereoselective way, one can vary the silyl group, i.e., the spectator-like organyl ligands around the silicon atom, and/or choose a silylating agent bearing a leaving group of proper reactivity. Our present work aims to make a contribution to a better understanding

the relationship between the nature of the leaving group and the silylating efficiency in the series of silylated cyclic urea derivatives.

Earlier Lane and Frye [2] reported on the preparation of several trimethylsilylated *N*-alkyl amides and the determination of their relative thermodynamical silylating abilities. These studies were stimulated by their experience that the silylated derivatives of pyrrolidone and ϵ -caprolactam exhibit grossly different reactivity, however, this phenomenon was not fully realised.

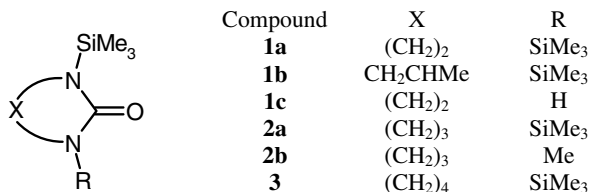
On the basis of their preliminary theoretical calculations, in a currently submitted paper Pongor et al. [3] studied the molecular structure of the trimethylsilylated *N,N*-dimethyl-carbamic acid and some of its analogue derivatives by ab initio quantum chemical methods. The high silylating power of compounds was explained by a strongly distorted (pseudo-) pentacoordinate

* Corresponding author. Tel.: +3612090555; fax: +3612090602.

E-mail address: szalayr@para.chem.elte.hu (R. Szalay).

environment around the silicon atom and the unusually long Si–O ester bond in molecules.

In a previous publication, we described the preparation of some *N*-trimethylsilylated cyclic ureas (**1a,b**, **2a,b** and **3**) resulting from the thermal decomposition of silylated dicarbamic acid derivatives [4].



Here, we discuss their *n*-octanolysis and molecular structure in correlation to their reactivity. The silylation reaction shown below was monitored by capillary gas chromatography



2. Results and discussion

2.1. Solvolysis study

Reaction rate measurements were carried out in tetrahydrofuran (THF) solutions containing the solvolysing agent, *n*-octanol (OctOH) in large excess relative to the concentration of the trimethylsilylated cyclic urea (TMSCU). In order to maintain the constant ionic strength in the course of reaction, lithium chloride was dissolved in medium as well (cf. [5]). The concentration vs time data were evaluated assuming a pseudo-first order kinetic model

$$-\frac{d[\text{TMSCU}]}{dt} = k[\text{OctOH}][\text{TMSCU}] = k_{\text{exp}}[\text{TMSCU}],$$

where k_{exp} is the pseudo-first order rate constant. The k_{exp} values were calculated from the integrated rate equation by exponential curve fitting (Microcal Origin 6.0)

$$[\text{TMSCU}] = [\text{TMSCU}]_0 e^{-k_{\text{exp}} t},$$

where $[\text{TMSCU}]_0$ denotes the initial concentration of substrate. In the followings the half-lives ($t_{1/2} = \ln 2/k_{\text{exp}}$) rather than the k_{exp} values themselves are used to characterise the reactivity of substrates.

As a preliminary experiment the hydrolysis of compounds was also investigated at ambient temperature. Our results revealed that there is a very large difference in the rates between the five- ($t_{1/2} \approx 10$ – 20 days for **1a,b**) and the six-/seven-membered ($t_{1/2} < 3$ min for **2a,b** and **3**) cyclic compounds. On the other hand, the hydrolytic reactivity of the open-chained analogue, *N,N'*-bis(trimethylsilyl)urea ($t_{1/2} \approx 25$ min), falls between those of the two former groups.

In order to adjust the solvolysis rate of the more reactive compounds low enough to follow the reaction conveniently by gas chromatography, *n*-octanol was selected as solvolysing agent in further experiments. Moreover, in contrast to the aqueous measurements the peak related to the silylated product, trimethylsilyloxyoctane (OctOTMS) is well separated from other peaks thus its area vs time data can be also evaluated in the calculations. The use of the more common and more volatile alcohols (methanol, ethanol, etc.) should be neglected from the same reason as in the case of water, however, the long retention time makes the heavier homologues also unfavourable. In turn secondary and tertiary alcohols are too inert to make difference in reactivity between substrates.

In Fig. 1 the relative concentration of the bis-silylated six-membered cyclic urea (**2a**) together with that of the solvolysis products as a function of time is shown. In the course of the reaction the amount of the monosilyl-urea as intermediate could be neglected all the time which is also indicated by the good linear correlation between the concentration of the bis-silylated substrate and the silyl-octanol (Fig. 2). However, in the case of the five-membered analogue (**1a**) the concentration of the monosilyl derivative (**1c**) remains constant for several weeks.

One can observe in Fig. 1 that the conversion related to the OctOTMS has already reached a value of 30% at the very first point of measurement (at $t = 0.7$ min). We explained this behaviour by the fact that despite of its short time (< 1 s) spent in the injector unit the sample got extensively decomposed to produce OctOTMS at the high injector temperature (250 °C) while no jump in conversion could be observed in the reaction of the much less reactive five-membered analogues (**1a,b**). In order to gain more evidence for this assumption therefore instead of withdrawing samples intermittently from the same reaction mixture we did as usual, 10 vials

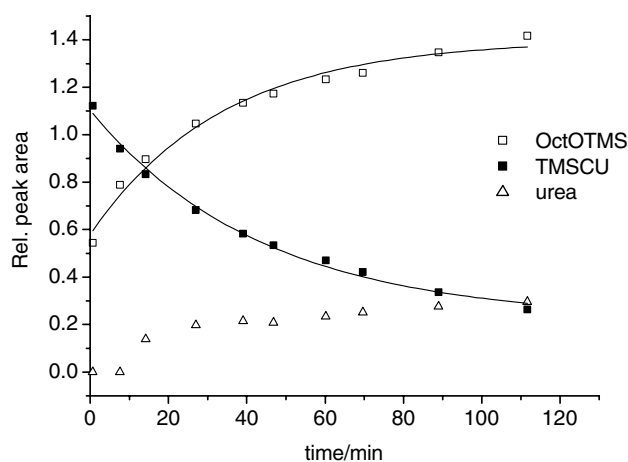


Fig. 1. The conversion plots for the *n*-octanolysis of **2a**.

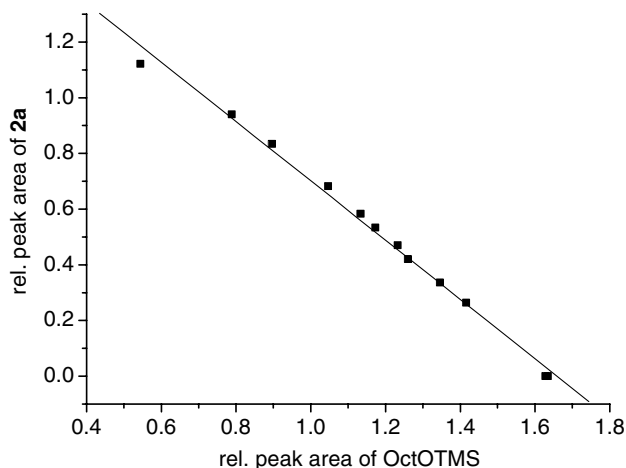


Fig. 2. The correlation between the momentary concentration of **2a** and the trimethylsilyloxyoctane during the solvolysis.

containing the reaction mixture of the same initial composition were run simultaneously. During the solvolysis each vial was once sampled for analysis at a recorded point of time (Method 1) and then its content was abruptly quenched at an also well-defined moment by adding large excess of methanol or water to decompose the remaining TMSCU. After standing for 2–3 h samples were again withdrawn from the mixtures to analyse them by gas chromatography (Method 2). Of course, in further measurements we checked the stability of the quenched mixtures and concluded that there was no observable change in the concentration of the OctOTMS upon standing for several days.

In accordance to the discussion above, the following kinetic model is suggested for the formation of the OctOTMS:

(Method 1) without quenching the mixtures:

$$[\text{OctOTMS}] = [\text{OctOTMS}]_{\infty} (1 - ae^{-k_{\text{exp}}t}),$$

$$a \equiv e^{-k^*t^*}, \quad 0 < a < 1,$$

where the ∞ symbol refers to the final value of concentration, k^* and t^* are the hypothetical rate constant and residence time of the sample in the hot injector;

(Method 2) with quenching the mixtures:

$$[\text{OctOTMS}] = [\text{OctOTMS}]_{\infty} (1 - e^{-k_{\text{exp}}t}).$$

It should be mentioned that in both cases the data were evaluated by curve fitting with three variable parameters (i.e., the values of $[\text{OctOTMS}]_{\infty}$, k_{exp} and a), however, in the Method 2 the value of a was identical to the unity within the experimental error (Fig. 3).

The half-lives of compounds listed in Table 1 point out the similar great difference between their reactivities

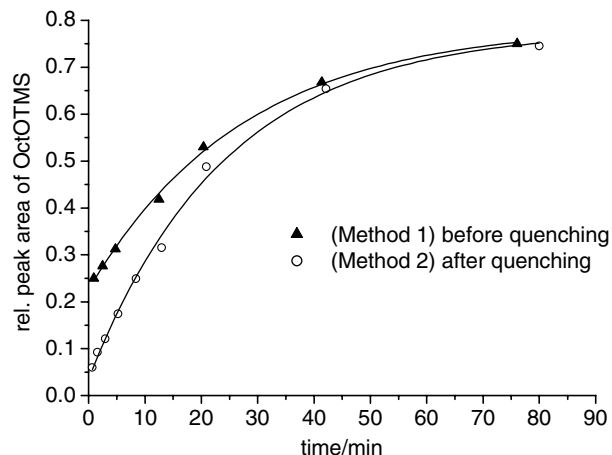


Fig. 3. The conversion plots for the *n*-octanolysis of **2a** using two different sampling methods (see details in the text).

Table 1

The half-lives of the *n*-octanolysis for **1a,b**, **2a,b** and **3**

Compound	1a	1b	2a	2b	3
$t_{1/2}$:	35 days	20 days	17 min	20 min	16 min

as observed in the hydrolysis. The octanolysis rate of the six- and the seven-membered cyclic silylated ureas (**2a,b**, **3**) is more than three orders of magnitude higher than that of the five-membered rings (**1a,b**).

2.2. Molecular structure studies

In order to elucidate the role of the structural features that govern the reactivity of compounds, the molecular structure of the five- (**1a-c**) and six- (**2a**) membered rings was determined by single-crystal X-ray diffraction method. The crystals of **1c** as a hydrolysis by-product precipitated from the mother liquor of **1a** upon long standing. Since no attempts were successful to obtain crystals from the oily seven-membered analogue (**3**) and the *N*-trimethylsilyl-*N'*-methyl six-membered derivative (**2b**), respectively, their structures were investigated by quantum chemical methods. However, theoretical calculations were also effected in the case of **1a** and **2a** in order to use a consistent set of geometrical data for all the relevant compounds.

Selected geometrical data listed in Tables 2 and 3 reveal that the experimental (i.e., solid phase) geometries agree well with the calculated (i.e., gas phase) ones thus the crystal packing forces have no significant influence upon the structure of molecules. In the crystal phase of the N-H compound (**1c**) two molecules constitute a centrosymmetric dimer via intermolecular N-H...O hydrogen bonds.

It is apparent that the arrangement of the non-hydrogen atoms is dominated by a plane involving the urea skeleton together with the C and Si atoms directly

Table 2
Selected X-ray crystallographic data for **1a–c** and **2a** (with e.s.d's in parentheses)

Compound	1a	1b	1c	2a
<i>Bond lengths (Å)</i>				
Si1–N1	1.739(7)	1.745(3) ^a	1.738(4)	1.761(4)
Si1–C6	1.825(12)	1.843(6) ^a	1.834(5)	1.848(7)
Si1–C5	1.830(10)	1.833(6) ^a	1.830(5)	1.859(7)
Si1–C4	1.849(11)	1.846(7) ^a	1.854(5)	1.861(7)
N1–C1	1.369(6)	1.377(5) ^a	1.356(5)	1.359(6)
N1–C2	1.444(12)	1.453(7) ^a	1.470(6)	1.469(6)
O1–C1	1.209(11)	1.220(7)	1.234(5)	1.247(5)
Si2–N2	1.737(6)	1.745(3)		1.758(5)
Si2–C8	1.812(11)	1.833(6)		1.841(6)
Si2–C9	1.835(11)	1.843(6)		1.846(7)
Si2–C7	1.852(11)	1.846(7)		1.858(5)
N2–C1	1.375(7)	1.377(5)	1.321(5)	1.365(6)
N2–C3	1.446(11)	1.453(7)	1.428(6)	1.466(6)
<i>Bond angles (°)</i>				
N1–Si1–C6	109.7(4)	109.4(2) ^a	110.2(2)	110.5(3)
N1–Si1–C5	109.9(4)	110.7(2) ^a	108.6(2)	112.3(3)
C6–Si1–C5	109.9(6)	109.5(3) ^a	111.7(3)	112.2(3)
N1–Si1–C4	105.6(5)	106.9(3) ^a	105.7(2)	106.0(3)
C6–Si1–C4	111.5(4)	110.4(4) ^a	109.5(3)	108.0(3)
C5–Si1–C4	110.1(5)	109.9(3) ^a	111.0(3)	107.5(3)
C1–N1–C2	110.4(4)	108.7(4) ^a	109.0(3)	119.0(5)
C1–N1–Si1	122.1(5)	122.6(3) ^a	125.2(3)	116.4(3)
C2–N1–Si1	127.5(2)	128.4(3) ^a	125.1(3)	124.4(4)
O1–C1–N1	124.9(4)	124.8(3) ^a	124.1(4)	118.6(5)
N1–C1–N2	110.0(6)	110.3(5)	110.5(4)	122.7(5)
N2–Si2–C8	110.7(4)	110.7(2)		111.1(3)
N2–Si2–C9	109.5(3)	109.4(2)		110.8(3)
C8–Si2–C9	109.8(6)	109.5(3)		112.1(3)
N2–Si2–C7	105.2(5)	106.9(3)		106.0(3)
C8–Si2–C7	110.6(4)	109.9(3)		108.5(3)
C9–Si2–C7	110.8(5)	110.4(4)		108.1(3)
C1–N2–C3	110.4(4)	108.7(4)	113.6(3)	119.7(5)
C1–N2–Si2	123.0(5)	122.6(3)		116.4(3)
C3–N2–Si2	126.5(2)	128.4(3)		123.9(4)
O1–C1–N2	125.1(4)	124.8(3)	125.4(3)	118.7(5)
<i>Torsion angles (°)</i>				
C6–Si1–N1–C1	–54.7(4)	–64.6(4) ^a	–47.8(4)	–64.1(5)
C5–Si1–N1–C1	66.2(5)	56.1(4) ^a	74.8(4)	62.1(5)
C4–Si1–N1–C1	–175.1(3)	175.8(4) ^a	–166.0(4)	179.2(4)
C6–Si1–N1–C2	122.3(4)	108.5(6) ^a	142.6(4)	111.5(6)
C5–Si1–N1–C2	–116.8(5)	–130.8(5) ^a	–94.8(4)	–122.4(6)
C4–Si1–N1–C2	2.0(4)	–11.1(6) ^a	24.4(4)	–5.2(6)
C8–Si2–N2–C1	52.7(4)	56.1(4)		60.6(5)
C9–Si2–N2–C1	–68.5(5)	–64.6(4)		–64.7(5)
C7–Si2–N2–C1	172.3(3)	175.8(4)		178.2(4)
C8–Si2–N2–C3	–131.0(4)	–130.8(5)		–118.7(6)
C9–Si2–N2–C3	107.8(6)	108.5(6)		116.0(6)
C7–Si2–N2–C3	–11.4(4)	–11.1(6)		–1.0(7)
C2–N1–C1–O1	178.4(4)	–175.4(3) ^a	177.4(4)	–179.4(6)
Si1–N1–C1–O1	–4.1(6)	–1.1(4) ^a	6.4(6)	–3.6(8)
C3–N2–C1–O1	–174.9(4)	–175.4(3)	–178.1(4)	179.3(6)
Si2–N2–C1–O1	1.9(6)	–1.1(4)		0.1(7)
<i>Interatomic distances (Å)</i>				
Si1...O	3.023	3.05 ^a	3.078	2.783
Si2...O	3.052	3.05		2.787

Molecule numbering as in Fig. 4.

^a A crystallographic twofold axis lying on the C1=O1 bond of **1b** generates atoms N1, Si1, C2, C4, C5 and C6.

Table 3
Selected geometrical data calculated for **1a**, **2a,b** and **3**

Compound	1a	2a	2b	3 (C ₂)	3 (C _s)
<i>Bond lengths (Å)</i>					
Si1–N1	1.787	1.805		1.804	1.816
Si1–C6	1.884	1.886		1.884	1.887
Si1–C5	1.884	1.885		1.887	1.887
Si1–C4	1.890	1.896		1.896	1.899
N1–C1	1.385	1.381	1.381	1.389	1.382
N1–C2	1.464	1.470	1.457	1.477	1.472
O1–C1	1.232	1.244	1.238	1.241	1.249
Si2–N2	1.787	1.805	1.803	1.804	1.816
Si2–C8	1.884	1.886	1.886	1.887	1.887
Si2–C9	1.884	1.885	1.885	1.884	1.887
Si2–C7	1.890	1.896	1.897	1.896	1.899
N2–C1	1.385	1.381	1.387	1.389	1.382
N2–C3	1.464	1.470	1.467	1.477	1.472
<i>Bond angles (°)</i>					
N1–Si1–C6	109.5	111.1		109.6	111.9
N1–Si1–C5	109.5	111.3		111.9	111.9
C6–Si1–C5	111.1	112.3		112.2	112.8
N1–Si1–C4	105.4	105.3		106.1	106.0
C6–Si1–C4	110.6	108.2		108.0	106.9
C5–Si1–C4	110.6	108.3		108.8	106.9
C1–N1–C2	110.7	121.0	124.3	119.6	124.7
C1–N1–Si1	121.2	115.0		115.2	112.1
C2–N1–Si1	128.0	123.9		121.5	123.3
O1–C1–N1	124.9	119.4	121.6	120.4	117.5
N1–C1–N2	110.3	121.2	118.7	119.1	125.0
N2–Si2–C8	109.5	111.1	111.5	111.9	111.9
N2–Si2–C9	109.5	111.3	111.1	109.6	111.9
C8–Si2–C9	111.1	112.3	112.2	112.2	112.8
N2–Si2–C7	105.4	105.3	105.3	106.1	106.0
C8–Si2–C7	110.6	108.2	108.1	108.8	106.9
C9–Si2–C7	110.6	108.3	108.2	108.0	106.9
C1–N2–C3	110.7	121.0	120.5	119.6	124.7
C1–N2–Si2	121.2	115.0	114.6	115.2	112.1
C3–N2–Si2	128.0	123.9	124.4	121.5	123.3
O1–C1–N2	124.9	119.4	119.7	120.4	117.5
<i>Torsion angles (°)</i>					
C6–Si1–N1–C1	–61.0	–62.4		–52.7	–64.0
C5–Si1–N1–C1	61.0	63.6		72.4	63.7
C4–Si1–N1–C1	180.0	–179.3		–169.1	179.8
C6–Si1–N1–C2	119.0	113.6		149.3	114.5
C5–Si1–N1–C2	–119.0	–120.4		–85.6	–117.8
C4–Si1–N1–C2	0.0	–3.3		33.0	–1.7
C8–Si2–N2–C1	61.0	62.4	63.1	72.4	64.0
C9–Si2–N2–C1	–61.0	–63.6	–62.9	–52.7	–63.7
C7–Si2–N2–C1	180.0	179.3	–179.9	–169.1	–179.8
C8–Si2–N2–C3	–119.0	–113.6	–109.2	–85.6	–114.5
C9–Si2–N2–C3	119.0	120.4	124.8	149.3	117.8
C7–Si2–N2–C3	0.0	3.3	7.8	33.0	1.7
C2–N1–C1–O1	180.0	–177.9	179.2	143.5	–179.2
Si1–N1–C1–O1	0.0	–1.8		–14.9	–0.7
C3–N2–C1–O1	180.0	177.9	172.9	143.5	179.2
Si2–N2–C1–O1	0.0	1.8	0.3	–14.9	0.7
<i>Interatomic distances (Å)</i>					
Si1···O	3.06	2.81		2.86	2.70
Si2···O	3.06	2.81	2.81	2.86	2.70

Molecule numbering as in Fig. 4.

bound to the nitrogens as well as one of the three C atoms of the Me₃Si group farthest away from the carbonyl group (i.e., C4 and C7, respectively, see Fig. 4).

As a consequence the ring atoms of the five-membered cyclic compounds are coplanar while in the six-membered rings only the outermost C atom relative to

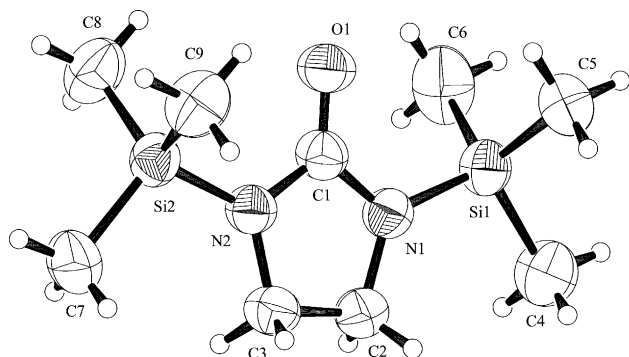


Fig. 4. X-ray structure and molecule numbering of **1a**. Atomic displacement ellipsoids are drawn at 30% probability level.

the carbonyl group moves out the plane of the ring. In terms of torsional angles, however, in the mixed silyl methyl six-membered derivative of C_1 symmetry (**2b**) the 'intraplanar' torsion angles involving all the aforementioned non-H atoms are planar to within 8° , while those excluding the *N*-methyl C atom and the ring C atom attached to the silylated nitrogen, respectively, are planar to within 1° . In the case of the seven-membered cyclic compound (**3**) two conformations with slightly different minimum energy (of C_2 symmetry with lower and of C_s symmetry with higher energy, respectively; $\Delta E = 3.8 \text{ kcal mol}^{-1}$) were found in the quantum chemical calculations. The structure of the C_s conformer can be interpreted in an analogous way like in the case of the bis-silylated six-membered ring, however, here two outermost ring carbons are present that are moving out of the plane to the same extent. In contrast to this, in the C_2 conformer it is the two ring carbon atoms attached to the nitrogens which strongly deviate from the planarity resulting in a slight pyramidality on the

N atoms as well. At the same time the dihedral angle between the N–Si bond and the planar urea moiety increases by a value of 15° .

It is worth comparing the values of the N–Si bond length as this bond of substrates ruptures in the solvolysis reaction. In the less reactive five-membered compounds this bond is ca. 0.02 \AA shorter than that of the more reactive six- and seven-membered analogues. In correlation to this, the *s* character of the nitrogen in the N–Si bond as determined by the natural population analysis (NPA) was found to be higher in the five-membered ring than in the six-/seven-membered analogues: the hybridisation state of N is $sp^{1.69}$ in **1a**, $sp^{1.91}$ in **2a**, $sp^{1.89}$ in **2b**, $sp^{1.93}$ in **3** of C_2 symmetry and $sp^{1.97}$ in **3** of C_s symmetry, respectively. On the other hand, the calculated partial charge on the Si atom in **1a** is less positive (1.975) than in the other homologues (1.981 for **2a**, 1.982 for **2b**, 1.979 for **3** of C_2 symmetry and 1.981 for **3** of C_s symmetry) resulting in a less favourable nucleophilic attack on the silicon.

It is also remarkable that in all compounds the Si...O (carbonyl) distance being much shorter than the sum of the van der Waals radii (3.6 \AA) [6], is longer by $0.2\text{--}0.3 \text{ \AA}$ in the five-membered rings than in the six- and seven-membered ones. Hence in the latter group of compounds a slight distortion of the geometry around the Si atom from a pure tetrahedron to a (pseudo-) trigonal bipyramid (TBP) is more expected (cf. [3]). In accordance to this the carbonyl oxygen and the methyl carbon of the TMS group lying in the plane of the molecule (C4, C7) occupy the pseudo-apical positions while the nitrogen and the other two methyl carbons do the pseudo-equatorial sites. The O...Si–C apical angle (180° for an ideal TBP) as well as the sum of the equatorial angles (360° for an ideal TBP) and the distance of the Si atom

Table 4
Characteristic data related to the pseudo-pentacoordination in **1a–c**, **2a,b** and **3**

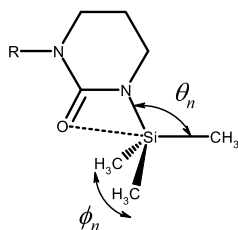
Compound	1a		1b	1c	2a		2b	3 (C_2)	3 (C_s)
	exp.	calc.	exp.	exp.	exp.	calc.	calc.	calc.	calc.
<i>Pseudo-apical angle</i> ($^\circ$)									
O...Si1–C4	154.2	154.4	155.1 ^a	149.4	159.4	159.0		158.7	161.6
O...Si2–C7	152.8	154.4	155.1		159.6	159.0	159.1	158.7	161.6
<i>Sum of the pseudo-equatorial angles</i> ($^\circ$)									
$\sum \phi_n(\text{Si1})$	329.5	330.0	329.6 ^a	330.5	335.0	334.8		333.6	336.6
$\sum \phi_n(\text{Si2})$	330.0	330.0	329.6		334.0	334.8	334.8	333.6	336.6
<i>Displacement of Si atom out of the pseudo-equatorial plane</i> (\AA)									
$\Delta(\text{Si1})$	0.589	0.600	0.591 ^a	0.579	0.537	0.551		0.564	0.531
$\Delta(\text{Si2})$	0.580	0.600	0.591		0.547	0.551	0.550	0.564	0.531
<i>Percentage of the trigonal bipyramidal</i> (%)									
% TBP _a (Si1)	2.1	3.0	2.1 ^a	3.8	11.8	11.4		9.3	14.9
% TBP _a (Si2)	3.1	3.0	2.1		9.9	11.4	11.5	9.3	14.9
% TBP _e (Si1)	3.5	5.2	3.8 ^a	6.6	20.9	20.1		16.6	26.1
% TBP _e (Si2)	5.1	5.2	3.8		17.7	20.1	20.3	16.6	26.1

Molecule numbering as in Fig. 4.

^a A crystallographic twofold axis lying on the C1=O1 bond of **1b** generates atoms N1, Si1, C2, C4, C5 and C6.

from the plane defined by the three equatorial atoms (zero for an ideal TBP) are shown in Table 4.

Furthermore, following Tamao et al. [7], we also calculated the percentage of TBP using formulas below (note that the second one misprinted in [7,8]):



$$\% \text{TBP}_a = \frac{109.5^\circ - \frac{1}{3} \left(\sum_{n=1}^3 \theta_n \right)}{109.5^\circ - 90^\circ} \times 100$$

$$\% \text{TBP}_e = \frac{\frac{1}{3} \left(\sum_{n=1}^3 \phi_n \right) - 109.5^\circ}{120^\circ - 109.5^\circ} \times 100$$

where θ_n and ϕ_n ($n = 1-3$) denote the three apical-to-equatorial and the three equatorial-to-equatorial bond angles, respectively. Comparison of the %TBP values as well as the other characteristic data listed in Table 4 indicates that the pseudo-pentacoordination around the Si atom is more pronounced in the more reactive six-/seven-membered rings than in the less reactive five-membered analogues.

In nucleophilic substitution reactions the increased reactivity of pentacoordinate silicon over tetracoordinate is well documented in the organosilicon chemistry literature [9]. Theoretical studies have pointed out that the positive charge on the central silicon atom is not only maintained but may well be increased by coordination of an additional ligand, even when the ligand is anionic [10]. Lengthening of bonds, particularly axial bonds, in pentacoordinate silicon species compared to tetracoordinate one was also shown. In general, pentacoordinate silicon complexes with a bidentate ligand have a five-membered chelate cycle and only few exceptions are known with smaller (four-membered) chelate cycles [11].

However, in silylated carbamic acid derivatives Pongor et al. [3] concluded on a weak through-space interaction of $\text{Si} \cdots \text{O}$ and $\text{Si} \cdots \text{N}$ type as a part of SiOC(O) and SiOC(N) four-membered cycles resulting in a strongly distorted (pseudo-) trigonal bipyramid environment around the silicon centre. In accordance to these, our results clearly manifest that the higher solvolysis rate of compounds can be similarly related to the higher extent of pseudo-pentacoordination around the silicon atom of a SiNC(O) chelate cycle in substrates. Hence our simple static (structure-based) model established essentially for the interpretation of the high silylating power of silylated carbamic acid esters and related compounds [3] is also valid for *N*-silylated cyclic ureas.

3. Conclusion

The structure and reactivity of pentacoordinate organosilicon compounds has attracted a great deal of interest mainly for their enhanced reactivity in nucleo-

philic substitution reactions [8,12]. However, from this point of view, only little attention was paid for the essentially tetracoordinate silicon derivatives with some pseudo-pentacoordinate character [13]. From our results, we concluded on the importance of this phenomenon in the silylating power of silylated cyclic urea derivatives. This work can be advanced by designing analogue molecules of intermediate and of extreme reactivity relative to that of the above mentioned derivatives. On the other hand, we are currently investigating model compounds containing biologically important five- and six-membered heterocycles (e.g. uric acid derivatives) with respect to their selective silylation/desilylation.

4. Experimental details

All operations were carried out under moisture-free conditions.

The preparation, the physical and spectroscopic data of the silyl-ureas **1a,b**, **2a,b** and **3** are discussed in [4]. Crystals of **1a** and **2a** suitable for X-ray diffraction study were obtained by vacuum sublimation. **1c** crystallised out as a by-product from the *n*-hexane solution of **1a**. The single crystal of **1b** formed upon cooling the residue of the thermal decomposition reaction.

4.1. Rate measurements

Tetrahydrofuran (Reanal) predried on KOH pellets was refluxed on potassium metal and then distilled. *n*-Octanol (Biogal) was boiled on calcium hydride before distillation. LiCl (Fluka) was heated in vacuum oven at 120 °C for several hours and then stored in a desiccator containing phosphorus pentoxide.

Each 0.5 ml portion of stock solution prepared from *n*-octanol, LiCl and internal standard (*n*-tridecane or *n*-tetradecane) in THF was transferred to screw-capped vial thermostated at 25.0 °C. In a typical run 30 μl of stock solution of substrate in THF was added to the solvolysing mixture via rubber septum. Thus, the initial concentration of substrate, octanol and LiCl was in order 1×10^{-3} , 2×10^{-1} and 2×10^{-2} mol dm^{-3} . Samples of 1 μl were periodically injected to the gas chromatograph (Chrompack CP 9000, 25 m \times 0.2 mm \times 0.33 μm HP Ultra-1 capillary column, He carrier gas, FID) so as to obtain at least 10 data points equally distributed over the 10–90% conversion range. Chromatographic peak areas were determined by the HP CHEMSTATION programme.

4.2. X-ray diffraction study

Single crystals of **1a–c** and **2a** were mounted in glass capillaries for X-ray data collection. For **1a** and **1c** data were collected on a Rigaku RAXIS-II imaging plate

Table 5
Crystal data of compounds **1a–c** and **2a**

	1a	1b	1c	2a
Empirical formula	C ₉ H ₂₂ N ₂ OSi ₂	C ₁₀ H ₂₄ N ₂ OSi ₂	C ₆ H ₁₄ N ₂ OSi	C ₁₀ H ₂₄ N ₂ OSi ₂
Formula weight	230.47	244.49	158.28	244.49
Crystal system	Monoclinic	Monoclinic	Monoclinic	Tetragonal
Space group	<i>P21/n</i>	<i>C2/c</i>	<i>P21/a</i>	<i>P4₁2₁2</i>
<i>a</i> (Å)	14.624(49)	21.6139(15)	11.345(5)	10.891(6)
<i>b</i> (Å)	6.459(54)	6.654(4)	6.410(4)	10.891
<i>c</i> (Å)	15.534(108)	12.4739(15)	12.898(4)	25.867(18)
α (°)	90	90	90	90
β (°)	102.51(36)	119.305(6)	100.40(3)	90
γ (°)	90	90	90	90
<i>V</i> (Å ³)	1432.4(162)	1564.3(9)	922.5(7)	3068(3)
<i>Z</i>	4	4	4	8
<i>D</i> _{calc} (g cm ⁻³)	1.069	1.038	1.140	1.059
μ (mm ⁻¹)	0.226	1.919	0.199	1.957
θ Range for data collection (°)	1.73–26.02	4.69–75.10	3.21–23.40	4.40–75.09
λ (Å)	0.71069	1.54178	0.71069	1.54178
Unique reflections collected	2699	1508	1308	1827
Observed reflections [<i>I</i> > 2 σ (<i>I</i>)]	1560	827	933	1005
Data/parameters/restraints	2694/130/12	1508/78/0	1308/95/0	1827/146/0
<i>R</i> ₁ [<i>I</i> > 2 σ (<i>I</i>)]	0.0807	0.0693	0.0703	0.0446
<i>wR</i> ₂ (all reflections)	0.2626	0.2496	0.2731	0.1345
Maximal/minimal $\Delta\rho$ (e Å ⁻³)	0.197/–0.214	0.490/–0.334	0.217/–0.204	0.214/–0.181

detector using graphite-monochromated Mo K α radiation at 293 K. For **1b** and **2a** data were collected on a Rigaku AFC6S diffractometer using graphite-monochromated Cu K α radiation at 293 K. Structure solutions with direct methods were carried out with the teXsan package [14]. The refinements were carried out using the SHELXL package [15] with full-matrix least-squares method on *F*². All non-hydrogen atoms were refined anisotropically. Hydrogen atoms were generated based upon geometric evidence and their positions were refined by the riding model. In the crystal structure of **1b** a crystallographic twofold axis lies on the the carbonyl moiety of the molecule. The methyl substituent of the five-membered ring, which does not fit the twofold symmetry, is disordered in the structure. In the crystal structure of **2a** the six-membered ring is present in its both sofa conformations due to disorder (the occupancies refined to 0.51928 and 0.48072). Crystallographic data for compound **1a–c** and **2a** are summarised in Table 5.

5. Computational details

Ground-state equilibrium geometries have been determined at the DFT level [16] using Becke's nonlocal three-parameter exchange functional [17] and the Lee–Yang–Parr correlation functional [18] (B3-LYP), supplemented by the 6-31G* basis set [19]. The aforementioned calculations were made by the GAUSSIAN 98 [20] suite of programmes. The natural population analysis (NPA) of Weinhold [21] was used in order to determine the *s* character of the nitrogen in the Si–N

bonds and interpret the one-electron density at the B3-LYP/6-31G* level. For compound **1a** C_{2v} symmetry was postulated. For **2a** and one conformer of **3** C_s, for the other conformer of the latter compound (**3**) C₂ symmetry was assumed. The equilibrium structure of **2b** was determined starting from the equilibrium ring structure of **2a** with a non-symmetric substitution.

6. Supplementary material

Crystallographic data for the structural analysis have been deposited with the Cambridge Crystallographic Data Centre, CCDC No. 244370 for compound **1a**, CCDC No. 244367 for compound **1b**, CCDC No. 244368 for compound **1c** and CCDC No. 244369 for compound **2a**. Copies of this information may be obtained free of charge from the Director, CCDC, 12 Union Road, Cambridge, CB2 1EZ, UK (fax: +44-1223-336033; e-mail: deposit@ccdc.cam.ac.uk or <http://www.ccdc.cam.ac.uk>).

Acknowledgements

R.Sz. wishes to thank Kornél Torkos for some gas chromatography mass spectrometric measurements and Ferenc Garay for the use of his PCICHEM programmes.

Authors thank the OTKA “Scientific Research Foundation of Hungary” (Grant Nos. F-030821 and T-037658) for the financial support.

References

- [1] (a) A.E. Pierce, *Silylation of Organic Compounds*, Pierce Chemical Co., Rockford, IL, 1968;
(b) G. van Look, G. Simchen, J. Heberle, *Silylating Agents*, Fluka Chemie AG, Buchs, Switzerland, 1995;
(c) M.T. El Gihani, H. Heaney, *Synthesis – Stuttgart* (1998) 357.
- [2] T.H. Lane, C.L. Frye, *J. Org. Chem.* 43 (1978) 4890.
- [3] (a) G. Pongor, K. Újszászy, Zs. Kolos, D. Knausz, in: XIth FECEM Conference on Organometallic Chemistry, Parma, Italy, 1995, Abstract, p. 218;
(b) G. Pongor, Zs. Kolos, R. Szalay, D. Knausz, *Pseudopentacoordination in silylcarbamates: structure-based prediction of silylating power*, doi:10.1016/j.theochem.2004.08.052.
- [4] R. Szalay, Zs. Böcskei, D. Knausz, Cs. Lovász, K. Újszászy, L. Szakács, P. Sohár, *J. Organomet. Chem.* 510 (1996) 93.
- [5] (a) R. Szalay, D. Knausz, L. Szakács, K. Újszászy, P. Sohár, *J. Organomet. Chem.* 487 (1995) 267;
(b) R. Szalay, D. Knausz, L. Szakács, K. Újszászy, B. Csákvári, P. Sohár, *J. Organomet. Chem.* 493 (1995) 267.
- [6] A. Bondi, *J. Phys. Chem.* 68 (1964) 441.
- [7] K. Tamao, T. Hayashi, Y. Ito, *Organometallics* 11 (1992) 2099.
- [8] D. Kost, I. Kalikhman, in: Z. Rappoport, Y. Apeloig (Eds.), *The Chemistry of Organic Silicon Compounds*, vol. 2, Wiley, New York, 1998, pp. 1339–1445 (Chapter 23).
- [9] A.R. Bassindale, S.J. Glynn, P.G. Taylor, in: Z. Rappoport, Y. Apeloig (Eds.), *The Chemistry of Organic Silicon Compounds*, vol. 2, Wiley, New York, 1998, pp. 495–511 (Chapter 9).
- [10] (a) J.A. Deiters, R.R. Holmes, *J. Am. Chem. Soc.* 112 (1990) 7197;
(b) M.S. Gordon, M.T. Carroll, L.P. Davis, L.W. Burggraf, *J. Phys. Chem.* 94 (1990) 8125.
- [11] (a) T. van den Ancker, B.S. Jolly, M.F. Lappert, C.L. Raston, B.W. Skelton, A.H. White, *J. Chem. Soc., Chem. Commun.* (1990) 1006;
(b) H.H. Karsch, F. Bienlein, A. Sladek, M. Heckel, K. Burger, *J. Am. Chem. Soc.* 117 (1995) 5160.
- [12] (a) C. Chuit, R.J.P. Corriu, C. Reye, J.C. Young, *Chem. Rev.* 93 (1993) 1371;
(b) R.R. Holmes, *Chem. Rev.* 96 (1996) 927;
(c) S.N. Tandura, M.G. Voronkov, N.V. Alekseev, *Topics in Current Chemistry*, vol. 131, Springer, Berlin, 1986, pp. 99–189;
(d) A.A. Macharashvili, V.E. Shklover, Yu.T. Struchkov, G.I. Oleneva, E.P. Kramarova, A.G. Shipov, Yu.I. Baukov, *J. Chem. Soc., Chem. Commun.* (1988) 683;
- (e) V.F. Sidorkin, V.V. Vladimirov, M.G. Voronkov, V.A. Pestunovich, *J. Mol. Struct. (Theochem)* 228 (1991) 1;
(f) A.G. Shipov, E.P. Kramarova, E.A. Mamaeva, O.A. Zamyshlyayeva, V.V. Negrebetsky, Yu.E. Ovchinnikov, S.A. Pogozhikh, A.R. Bassindale, P.G. Taylor, Yu.I. Baukov, *J. Organomet. Chem.* 620 (2001) 139;
(g) A.R. Bassindale, D.J. Parker, P.G. Taylor, N. Auner, B. Herrschaft, *J. Organomet. Chem.* 667 (2003) 66.
- [13] (a) W. Bett, S. Craddock, D.W.H. Rankin, *J. Mol. Struct.* 66 (1980) 159;
(b) I.S. Ignatyev, A.N. Lazarev, *Chim. Phys.* 10 (1983) 1315;
(c) I.S. Ignatyev, *J. Mol. Struct.* 245 (1991) 139;
(d) J. Rohonczy, D. Knausz, B. Csákvári, P. Sohár, I. Pelczer, L. Párkányi, *J. Organomet. Chem.* 340 (1988) 293;
(e) Zs. Böcskei, J. Rohonczy, R. Szalay, D. Knausz, *Acta Crystallogr. Sect. C* 52 (1996) 2063.
- [14] *teXsan, Crystal Structure Analysis Package*, Molecular Structure Co., 1985, 1992, Houston, TX.
- [15] G.M. Sheldrick, *SHELXL-97 Program for the Refinement of Crystal Structures*, University of Göttingen, 1997.
- [16] R.G. Parr, W. Yang, *Density Functional Theory of Atoms and Molecules*, Oxford, New York, 1989.
- [17] A.D. Becke, *J. Chem. Phys.* 98 (1993) 5648.
- [18] C. Lee, W. Yang, R.G. Parr, *Phys. Rev. B* 41 (1988) 785.
- [19] P.C. Hariharan, J.A. Pople, *Theor. Chim. Acta* 28 (1973) 213.
- [20] M.J. Frisch, G.W. Trucks, H.B. Schlegel, G.E. Scuseria, M.A. Robb, J.R. Cheeseman, V.G. Zakrzewski, J.A. Montgomery Jr., R.E. Stratmann, J.C. Burant, S. Dapprich, J.M. Millam, A.D. Daniels, K.N. Kudin, M.C. Strain, O. Farkas, J. Tomasi, V. Barone, M. Cossi, R. Cammi, B. Mennucci, C. Pomelli, C. Adamo, S. Clifford, J. Ochterski, G.A. Petersson, P.Y. Ayala, Q. Cui, K. Morokuma, D.K. Malick, A.D. Rabuck, K. Raghavachari, J.B. Foresman, J. Cioslowski, J.V. Ortiz, A.G. Baboul, B.B. Stefanov, G. Liu, A. Liashenko, P. Piskorz, I. Komaromi, R. Gomperts, R.L. Martin, D.J. Fox, T. Keith, M.A. Al-Laham, C.Y. Peng, A. Nanayakkara, C. Gonzalez, M. Challacombe, P.M.W. Gill, B. Johnson, W. Chen, M.W. Wong, J.L. Andres, C. Gonzalez, M. Head-Gordon, E.S. Replogle, J.A. Pople, *GAUSSIAN98, Revision A.7*, Gaussian, Inc., Pittsburgh, PA, 1998.
- [21] (a) A.E. Reed, R.B. Weinstock, F. Weinhold, *J. Chem. Phys.* 83 (1985) 735;
(b) NBO Version 3.1, E.D. Glendening, A.E. Reed, J.E. Carpenter, F. Weinhold.